PCCP

Cite this: *Phys. Chem. Chem. Phys.*, 2012, **14**, 2399–2407

www.rsc.org/pccp

PAPER

A study of the atmospherically important reactions of dimethylsulfide (DMS) with I_2 and ICl using infrared matrix isolation spectroscopy and electronic structure calculations

Sonya Beccaceci,[a] Nerina Armata,[a] J. Steven Ogden,†[a] John M. Dyke,*[a] Lydia Rhyman[b] and Ponnadurai Ramasami[b]

Received 27th October 2011, Accepted 13th December 2011
DOI: 10.1039/c2cp23392d

The reactions of dimethylsulfide (DMS) with molecular iodine (I_2) and iodine monochloride (ICl) have been studied by infrared matrix isolation spectroscopy by co-condensation of the reagents in an inert gas matrix. Molecular adducts of DMS + I_2 and DMS + ICl have also been prepared using standard synthetic methods. The vapour above each of these adducts trapped in an inert gas matrix gave the same infrared spectrum as that recorded for the corresponding co-condensation reaction. In each case, the infrared spectrum has been interpreted in terms of a van der Waals adduct, DMS : I_2 and DMS : ICl, with the aid of infrared spectra computed for their minimum energy structures at the MP2 level. Computed relative energies of minima and transition states on the potential energy surfaces of these reactions were used to understand why they do not proceed further than the reactant complexes DMS : I_2 and DMS : ICl. The main findings of this research are compared with results obtained earlier for the DMS + Cl_2 and DMS + Br_2 reactions, and the atmospheric implications of the conclusions are also considered.

Introduction

The sulfur cycle in the earth's atmosphere has been the subject of intense investigation in recent years because of the need to assess the contribution of anthropogenically produced sulfur to acid rain, visibility reduction and climate modification.[1–4] Roughly half of the global flux of sulfur is thought to be from natural sources and a significant fraction of all natural sulfur that enters the atmosphere arises from DMS being volatilized from the oceans.[5–7] It is produced by biodegradation of oceanic phytoplankton in ocean environments, initiated by ultraviolet (u.v.) radiation from the sun, as well as by anthropogenic activities. Oxidation of DMS in the atmosphere leads to formation of cloud condensation nuclei that reduce the solar radiation reaching the earth's surface. This reaction therefore plays a role in climate modification.

The main oxidants of DMS in the atmosphere are thought to be the OH radical during the day and the NO_3 radical at night.[8,9] However, oxidation of DMS appears to be more rapid than expected from OH and NO_3 reactions and other DMS oxidation reactions, involving atomic and molecular halogens and halogen monoxide radicals have been proposed.[10,11] It has been demonstrated in field measurements on I_2, OIO, IO and NO_3 that large concentrations of I_2 can occur in the marine boundary layer possibly arising from micro-algae at low tide.[12,13] Other sources of molecular iodine have been identified, notably the interaction of ozone with sea surfaces,[14,15] and the transformation of sea salt components into interhalogen negative ions such as I_2Cl^-, ICl_2^-, I_2Br^-, and IBr_2^- on freezing sea water.[16–18] On warming, these interhalogen ions are sources of the halogens and interhalogens I_2, Br_2, ICl, and IBr in the gas-phase, notably in the polar marine boundary layer.[16–18] Once formed, the diatomic halogens (*e.g.* I_2 and ICl from I_2Cl^- and ICl_2^-) can diffuse into the gas-phase yielding reactive halogen species to the atmosphere. Also, it has been demonstrated recently that $I_{2(g)}$ emissions from heterogeneous reactions of O_3 with $I^-_{(aq)}$ are significantly enhanced in the presence of surface active weak acids, under mildly acidic conditions that are typical of fine marine aerosols, and that similar enhancements are expected for $Cl_{2(g)}$ and $Br_{2(g)}$ from the interfacial reactions of O_3 with Cl^-(aq) and Br^-(aq) respectively.[19]

The reactions of DMS with I_2, ICl, and IBr, as well as IO, formed from the I + O_3 reaction, to give DMSO + I, provide important ways to link the global cycles of sulfur and iodine.[20,21] Hence any reliable model of DMS oxidation in the atmosphere must include reactions of DMS with halogens and interhalogens.

In recent work we have studied the mechanisms of the reactions of molecular chlorine and bromine with DMS using

[a] *School of Chemistry, University of Southampton, Southampton SO17 1BJ, UK*
[b] *Department of Chemistry, University of Mauritius, Réduit, Mauritius*
† Deceased.

infrared matrix isolation spectroscopy, u.v. photoelectron spectroscopy and electronic structure calculations.[22–24] In this present work, these studies are extended to the DMS + I_2 and DMS + ICl reactions. The aim is to determine the reaction mechanism and reaction products, and, if possible, identify reaction intermediates. It is also proposed to make a comparison with the results we obtained earlier for the DMS + Cl_2 and DMS + Br_2 reactions.[22–24]

Experimental

For the matrix isolation infrared spectroscopy experiments, a cryostat equipped with a CsI deposition window was used.[25] The inlet system used for the DMS + I_2 and DMS + ICl reactions was similar to that used previously in matrix isolation infrared and PES measurements on the DMS + Cl_2 and DMS + Br_2 reactions.[22–24] In this inlet system, the inner tube is movable with respect to the outer tube; in this way DMS and I_2 (or ICl), diluted in an inert gas were introduced *via* the inner and outer parts of the inlet tube respectively. The inner tube could be moved, in order to change the reaction distance (reaction time) to the CsI deposition window. Both nitrogen and argon (purities > 99.99%) were used as matrix gases, and cryogenic cooling was provided by an Air Products CSW-202 water cooled Displex closed cycle unit. In a typical co-condensation experiment, I_2 (or ICl) vapour diluted by a factor of 10 with argon or nitrogen, was allowed to mix with DMS vapour, also diluted with argon or nitrogen, in a region ~10 cm from the cold (12 K) deposition window. This flux was then co-condensed with more matrix gas (~x100) onto the cold window. The approximate dilution ratio in the matrix was 1 : 1000. Infrared spectra were recorded in the wavenumber range 4000–180 cm^{-1} using a data station to allow manipulation and storage of experimental data. The experimental resolution was typically 2 cm^{-1}.

UV photoelectron spectroscopy experiments were carried out using a 10 cm mean radius hemispherical analyser designed for the study of short-lived molecules.[26,27] A HeI (21.22 eV) photon source was used in these experiments. The experimental resolution was typically 25 meV (200 cm^{-1}). The inlet system used for these DMS + I_2 and DMS + ICl experiments was similar to that used in the matrix isolation infrared experiments.

The dark red 1 : 1 DMS : I_2 adduct was prepared using standard vacuum line procedures. In a typical synthesis, DMS and iodine with DMS slightly in excess (typically no more than 10% excess) were successively condensed into a tap ampoule at 77 K, and the mixture was slowly warmed to room temperature. The resulting reaction yielded a dark red liquid. Most of the excess DMS could be removed using freeze-pump-thaw cycles using suitable freezing mixtures. The vapour above the liquid obtained was investigated by matrix isolation infrared measurements. Sampling of this vapour into a photoelectron spectrometer through a needle valve showed only bands of DMS and I_2.[28,29] Similar experiments performed for DMS with ICl resulted in a brown-orange solid. The vapour above this solid was investigated by matrix isolation IR measurements. PES experiments performed on the vapour above this solid showed only signals of DMS, and ICl.[28,30,31]

Samples (obtained from Aldrich) of DMS (≥ 99%), I_2 (≥ 99.99%) and ICl (>98%) were used without further purification in these experiments.

Electronic structure calculations

All electronic structure calculations were performed using the Gaussian03 programme.[32] Minimum energy geometries and infrared spectra of the reactants, reaction intermediates and reaction products were computed. These calculations were carried out at the MP2 level of theory,[33] using cc-pVDZ basis sets[34] for all atoms except iodine for which the ECP basis set aug-cc-pVDZ + PP[35] taken from the EMSL basis set library has been used. All optimised structures gave real frequencies except for the transition states which have one imaginary frequency.

For the optimised geometries obtained for the van der Waals complexes DMS : I_2, DMS : ICl and DMS : Br_2, vertical transition energies were calculated with time dependent density functional theory (TDDFT) with the range-separated hybrid exchange correlation functional CAM-B3LYP.[36–39] This functional has different amounts of Hartree–Fock and Becke (B88) exchange at short and long range. It was designed to improve on the B3LYP description of long-range phenomena, such as charge–transfer excitation or polarizability and is known to be reliable for calculating vertical excitation energies for small molecules to within *ca.* 0.25 eV.[36–39]

Results

(i) Co-condensation infrared experiments: DMS with I_2 and DMS with ICl

Fig. 1(a) shows a typical infrared spectrum obtained from a DMS + I_2 co-condensation experiment in a nitrogen matrix. As was the case in the earlier DMS + Br_2 study,[24] characteristic new bands associated with a reaction intermediate were observed (at 1040 and 1331 cm^{-1}; see Fig. 1(b))) and several other absorptions of this reaction intermediate were virtually coincident with those of DMS. The spectra obtained corresponded to only a slight excess of DMS and this can be seen in Fig. 1(b) which shows a band of unreacted DMS at 1313 cm^{-1}.

A typical spectrum obtained from a DMS + ICl co-condensation experiment is shown in Fig. 2. As can be seen in Fig. 2(b), bands associated with a reaction intermediate were observed at 1040 and 1333 cm^{-1} and bands associated with unreacted DMS were seen at 1313 and 1032 cm^{-1}.

(ii) Infrared spectra recorded for the DMS : I_2 and DMS : ICl adducts

For the separately prepared adducts DMS : I_2 and DMS : ICl, a dark red liquid and a brown orange solid respectively at room temperature, matrix isolation infrared spectra were recorded in nitrogen matrices by sampling the vapour above each adduct. For the DMS : I_2 adduct the spectrum was the same as that shown in Fig. 1, showing product bands at 1040 and 1331 cm^{-1}. Matrix infrared spectra recorded for the vapour above the DMS : ICl adduct showed the bands observed at 1040 and 1333 cm^{-1} in the DMS and ICl

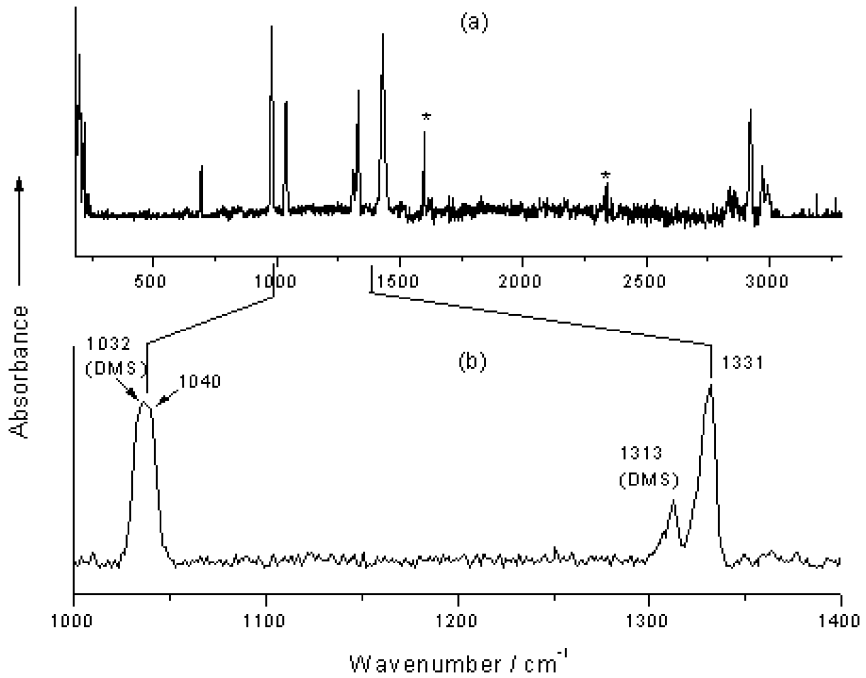

Fig. 1 Experimental DMS + I_2 spectrum recorded in a nitrogen matrix (a) in the 200–3200 cm^{-1} region, and (b) in the 1000–1400 cm^{-1} region; the two features labelled with a "*", in order of increasing wavenumber, are due to water and carbon dioxide.

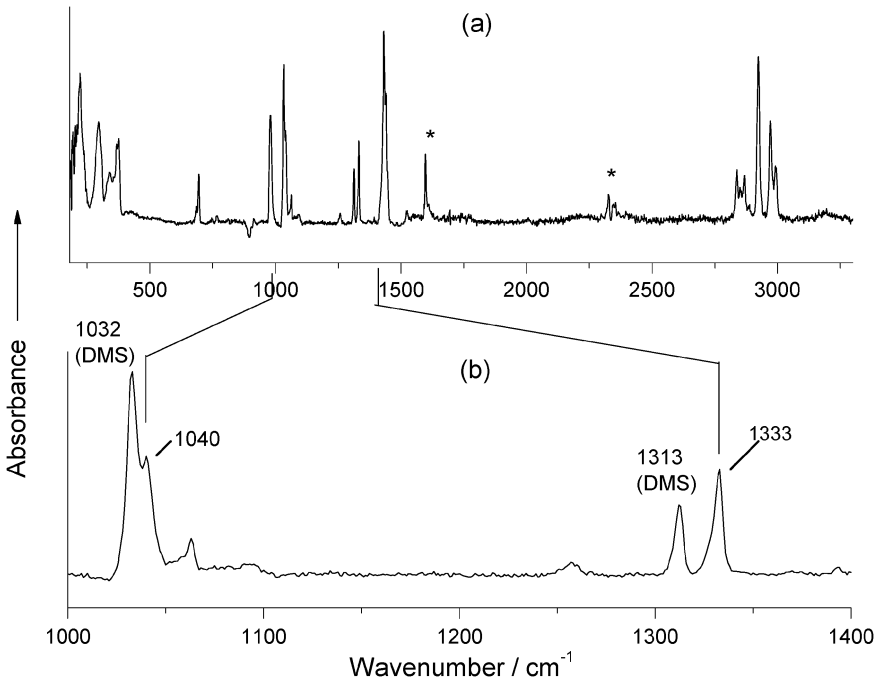

Fig. 2 Experimental DMS + ICl spectrum recorded in a nitrogen matrix (a) in the 200–3200 cm^{-1} region, and (b) in the 1000–1400 cm^{-1} region; the two features labelled with a "*", in order of increasing wavenumber, are due to water and carbon dioxide.

co-condensation experiments. Weak bands were also observed associated with monochloroDMS (CH_3SCH_2Cl; at 657, 702, 755, 983, 1234, 1429, 1444, 2851 and 2933 cm^{-1}) and HCl (at 2850 cm^{-1} [40]). These results were interpreted as the bands at 1040 and 1333 cm^{-1} being associated with the DMS : ICl complex. The bands associated with monochloroDMS and HCl arise from a small amount of dissociation of ICl into I_2 and Cl_2 with the Cl_2 reacting with DMS to give monochloroDMS and HCl,[22–24] and I_2 reacting with DMS to give the DMS : I_2 complex which is in much lower concentration than the DMS : ICl complex.

A comparison of the experimental infrared spectra obtained for the DMS : I_2 and DMS : ICl complexes with those computed at the MP2 level for the van der Waals and covalent structures in each case is shown in Fig. 3 and 4 respectively, as well as in Tables 1 and 2.

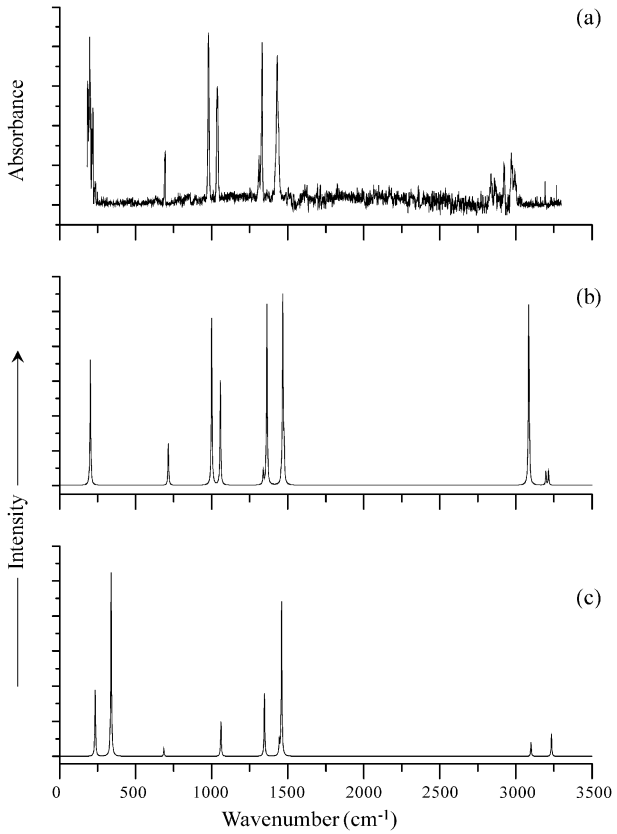

Fig. 3 Comparison of experimental and simulated spectra (a) (upper) DMS + I_2 experimental spectrum (b) (middle) Calculated for the van der Waals structure DMS : I_2 at the MP2 level, and (c) (lower) Calculated for the covalent structure Me_2SI_2 at the MP2 level (in this spectrum bands in the 500–3500 cm^{-1} region have been increased in intensity by ×5, to assist comparison with (a) and (b)); in the simulated spectra Lorentzian functions have been used with a half-width of 5 cm^{-1}.

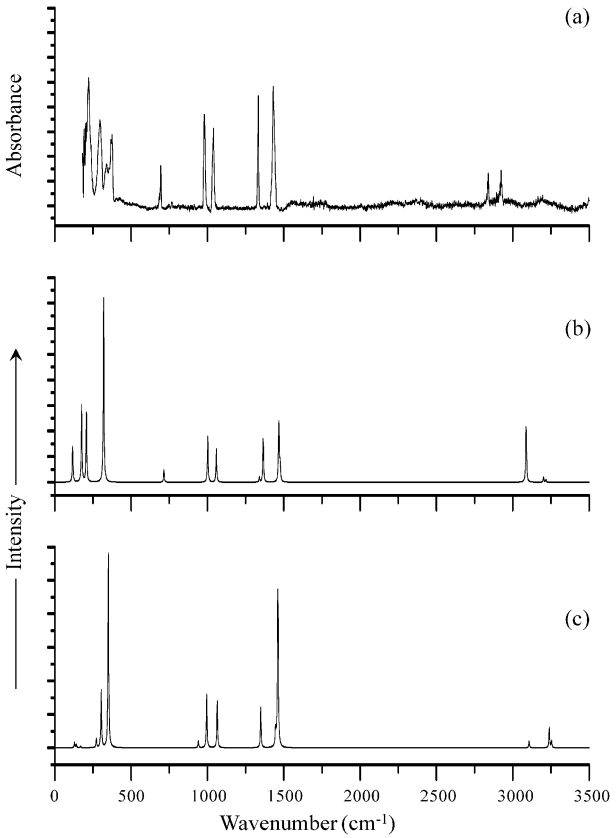

Fig. 4 Comparison of experimental and simulated spectra (a) (upper) DMS + ICl experimental spectrum (b) (middle) Calculated for the van der Waals structure DMS : ICl at the MP2 level, and (c) (lower) Calculated for the covalent structure Me_2SICl at the MP2 level (in this spectrum bands in the 500–3500 cm^{-1} region have been increased in intensity by ×10, to assist comparison with (a) and (b)); in the simulated spectra Lorentzian functions have been used with a half-width of 10 cm^{-1}.

(iii) Computed relative energies of minima and transition states for the DMS + I_2 and DMS + ICl reactions

As has been found for the DMS + X_2 reactions, where X = Cl or Br,[22–24] the potential energy surfaces for the DMS + XY reactions (where X and Y are halogen atoms) are similar in that they all show the same minima, with similar structures but different geometrical parameters, different relative energies and different potential energy barriers that interconnect them. The minima on each surface are:—the reagents, a reagent-like complex DMS : XY (which is termed a van der Waals structure in this work), a covalent structure Me_2SXY, a product-like complex MXDMS : HY and the products MXDMS + HY (where MXDMS = monohaloDMS). For DMS + I_2, the computed structures of the van der Waals and covalent structures at the MP2 level are shown in the top half of Fig. 5. The corresponding DMS : ICl structures are very similar and are shown in the lower half of Fig. 5. For the DMS : ICl van der Waals complex, the iodine atom is bound to the sulfur atom of DMS as shown in Fig. 5. This structure is lower in energy by 10.2 kcal mol^{-1} than the van der Waals structure DMS : ClI where the chlorine atom of the ClI unit is closer to the sulfur atom (the computed MP2 energies relative to the reagents are −14.49 and −4.24 kcal mol^{-1} respectively). For the reactions DMS + I_2 and DMS + ICl, the computed relative energies of the minima and the transition states that

Table 1 Experimental and calculated IR wavenumber values (cm^{-1}) for DMS + I_2

$Me_2S : I_2$ in a N_2 matrix Experimental	$Me_2S : I_2$ van der Waals complex Calc. at the MP2 level Most intense absorptions[a] (intensity/km mol^{-1})	Me_2SI_2 covalent complex Calc. at the MP2 level Most intense absorptions[a] (intensity/km mol^{-1})
	202(18)	234(47)
		339(131)
695(w)	715(6)	686(1)
979(m)	1000(24)	
1040(m)	1057(15)	1061(5)
	1339(2)	1347(9)
1331(m)	1363(26)	1444(2)
	1457(1)	1460(22)
1431(m)	1467(10)	
1441(m)	1468(18)	
	1476(5)	
2927(s)	3084(23)	
2972(m)	3088(9)	3100(2)
2994(m)	3197(2)	3234(3)
	3215(2)	

[a] Only the most intense calculated absorptions are listed.

Table 2 Experimental and calculated IR wavenumber values (cm^{-1}) for DMS + ICl van der Waals and covalent complexes

Me_2S : ICl in a N_2 matrix Experimental	Me_2S : ICl van der Waals complex Calc. at the MP2 level Most intense absorptions[a] (intensity/km mol^{-1})	Me_2SICl covalent complex Calc. at the MP2 level Most intense absorptions[a] (intensity/km mol^{-1})	Me_2S : ClI van der Waals complex Calc. at the MP2 level Most intense absorptions[a] (intensity/km mol^{-1})
			78(33)
	117(14)	129(8)	128(29)
	176(30)	141(5)	194(5)
	207(27)	169(2)	
		272(13)	268(1)
297(s)	320(72)	304(86)	316(50)
335(s)		351(290)	
685(w)	715(5)		724(3)
		940(1)	923(1)
		995(8)	1000(11)
980(m)	1002(18)	1064(7)	1056(12)
1040(m)	1058(13)		
	1340(2)		1340(5)
1333(m)	1365(17)	1349(6)	1366(11)
		1445(2)	
1432(s)	1466(11)	1448(1)	1471(15)
1449(s)	1469(18)	1460(16)	1474(11)
	1476(6)	1463(14)	1483(1)
2869(w)			3080(29)
2923(s)	3086(18)	3107(1)	3084(20)
2973(m)	3089(8)	3239(3)	3187(10)
2995(m)	3201(2)	3254(1)	
	3217(1)		3208(5)

[a] Only the most intense calculated absorptions are listed.

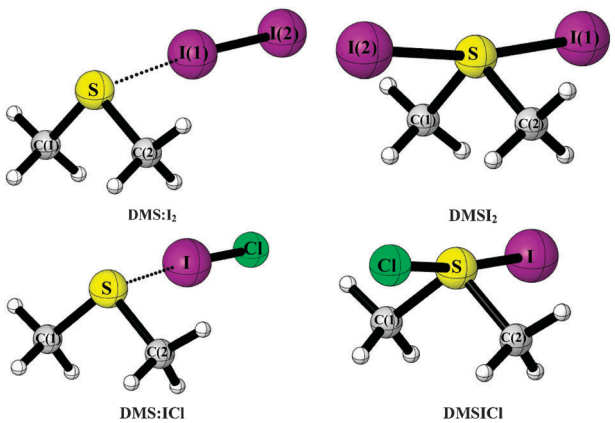

Fig. 5 Optimised MP2 structures at the MP2 level of DMS-I_2 and DMS-ICl. The structures on the left-hand side show the van der Waals structures; those on the right-hand side show the covalent structures.

connect them, computed at the MP2 level, are shown in Fig. 6(a) and 6(b) respectively. Fig. 6(a) shows that unlike the DMS + Br_2 reaction, the DMS + I_2 reaction to give the final products MIDMS + HI is endothermic (energy relative to the reagents +5.97 kcal mol^{-1}) whereas in the DMS + Br_2 case the reaction to give the final products MBrDMS + HBr is exothermic (relative energy −15.9 kcal mol^{-1}). The DMS + Cl_2 reaction to give MClDMS + HCl is even more exothermic (energy relative to reagents −35.0 kcal mol^{-1}). Also, unlike the DMS + Cl_2 and DMS + Br_2 reactions, the DMS + I_2 reaction has a van der Waals minimum lower in energy than that of the covalent structure (see Fig. 6). The barrier for interconversion of the van der Waals structure to the covalent structure is also much higher in the DMS + I_2 case than the DMS + Br_2 case (TS1 relative energies +28.3 kcal mol^{-1} for DMS + I_2 compared with +18.7 kcal mol^{-1} for DMS + Br_2 and +6.0 kcal mol^{-1} for DMS + Cl_2 at the MP2 level). Therefore, unlike the DMS + Cl_2 reaction but as was the case for the DMS + Br_2 reaction, at room temperature and at the lower temperatures of an inert gas matrix, the DMS + I_2 reaction is expected to stop at the formation of a van der Waals complex and not proceed further on the potential energy surface.

In the case of DMS + ICl, the reaction to produce MIDMS + HCl is exothermic (energy relative to the reagents is −14.6 kcal mol^{-1}). The alternative reaction product channel MClDMS + HI is less exothermic (energy relative to the reagents −9.7 kcal mol^{-1}). As can be seen in Fig. 6(b), the van der Waals complex is lower in energy than the covalent structure, and the potential barrier for conversion to the covalent structure is high (TS1 relative energy +27.4 kcal mol^{-1}) as is the case for the DMS + I_2 reaction (TS1 relative energy +28.2 kcal mol^{-1}). The DMS + I_2 and DMS + ICl reactions are not therefore expected to proceed further than the van der Waals complex. The structure of the DMS : ICl complex has the iodine atom closer to the sulfur atom of DMS as shown in Fig. 5. A comparison of the structural parameters computed at the MP2 level for the Me_2S : I_2 van der Waals complex and the Me_2SI_2 covalent complex is given in Table 3(a), and a similar comparison for Me_2S : ICl, Me_2S : ClI and Me_2SICl is given in Table 3(b).

(iv) Comparison of experimental spectra with computed infrared spectra of possible reaction intermediates and products

For the DMS + I_2 reaction, the infrared spectra for MIDMS and the product-like complex MIDMS : HI showed poor agreement with the spectrum shown in Fig. 1 and 3(a) indicating that it is probably associated with either a van der Waals

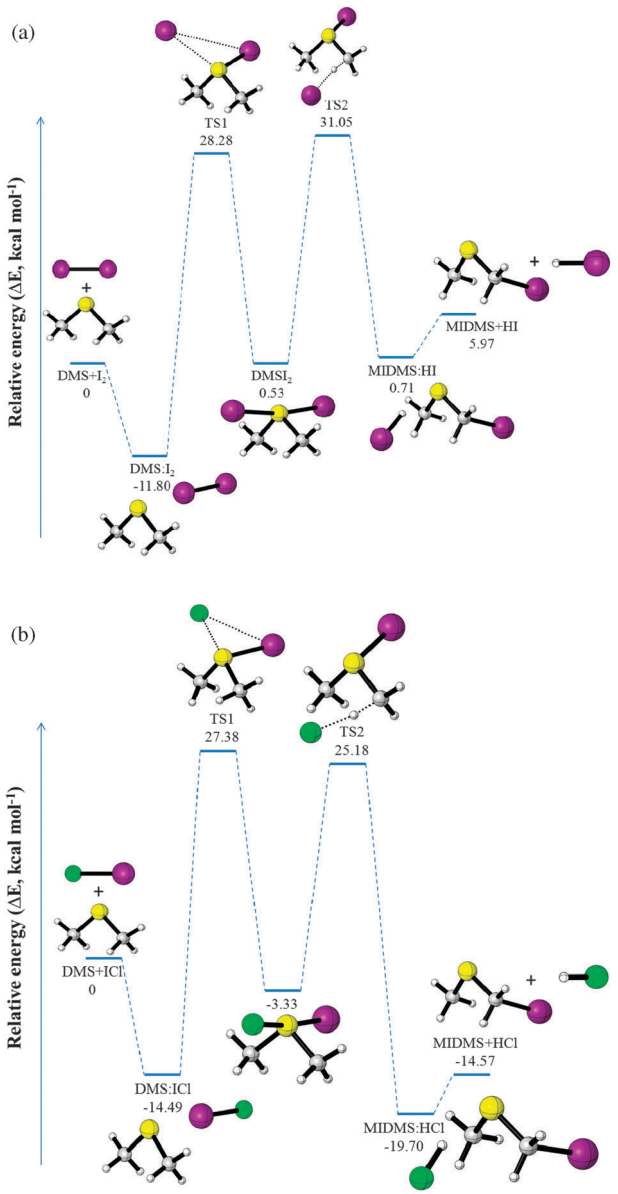

Fig. 6 Relative energy level diagrams calculated at the MP2 level for (a) DMS + I_2 (upper) and (b) DMS + ICl (lower).

complex DMS : I_2 or a covalent structure Me_2SI_2 which contains a central S atom covalently bound to two I atoms and two methyl groups (see Fig. 5). Both structural types have been observed in earlier studies by our group. The van der Waals structure has been observed in matrix isolation infrared studies of the DMS + Cl_2 and the DMS + Br_2 reactions[24] and the covalent structure Me_2SCl_2 has been observed as a reaction intermediate in studies of the DMS + Cl_2 reaction in the gas-phase by PES.[22,23] The experimental infrared spectrum obtained for the DMS + I_2 reaction is compared with the computed infrared spectra for the van der Waals complex DMS : I_2 and the covalent structure Me_2SI_2 in Fig. 3. Fig. 3(a) shows the experimental spectrum, and Fig. 3(b) and (c) show the computed spectra for the van der Waals complex and the covalent structure respectively. As shown in Fig. 3 and Table 1, the agreement for the experimental band positions and relative intensities is much better for the van der Waals

Table 3 (a) Structural parameters computed at the MP2 level for the minimum energy geometries of (i) the $Me_2S : I_2$ van der Waals complex, (ii) the Me_2SI_2 covalent complex[a]; (b) Structural parameters computed at the MP2 level for the minimum energy geometries of (i) the Me_2S : ICl van der Waals complex, (ii) the Me_2SICl covalent complex, and the Me_2S : ClI van der Waals complex

	(i) van der Waals complex	(ii) covalent complex[a]
Bond lengths/angstrom		
C(1)–S	1.816 (1.815)[b]	1.832
C(2)–S	1.816 (1.815)	1.832
S–Br(1)	2.969 (2.724)	2.772
I(1)–I(2)	2.791 (2.436)	—
Angles/deg.		
C(1)–S–C(2)	99.0 (99.1)	99.3
C(1)–S–I(1)	96.4 (95.4)	93.0
C(2)–S–I(1)	96.4 (95.4)	93.0
S–I(1)–I(2)	175.1 (175.1)	—

	Me_2S : ICl van der Waals complex	Me_2SICl covalent complex	Me_2S : ClI van der Waals complex
Bond lengths/angstrom			
C(1)–S	1.816	1.827	1.814
C(2)–S	1.816	1.827	1.814
S–I(1)	2.881	2.743	—
I–Cl	2.444	—	2.408
S–Cl	—	2.344	2.989
Angles/deg.			
C(1)–S–C(2)	99.1	100.0	98.3
C(1)–S–I	97.3	92.7	—
C(2)–S–I	97.3	92.7	—
S–I–Cl	175.8	—	—
S–Cl–I	—	—	172.3
C(1)–S–Cl	—	91.3	90.5
C(2)–S–Cl	—	91.3	90.5

[a] See Fig. 5 for the atom numbering used. [b] Computed values for the $Me_2S : Br_2$ van der Waals complex at the MP2 level; see ref. 24.

structure than the covalent structure, particularly in the 900–1500 cm^{-1} region. The computed wavenumber values for the van der Waals structure are slightly higher than the experimental values because only harmonic values have been calculated and because only partial allowance has been made for electron correlation in the MP2 calculations. These calculations indicate that the 1040 and 1331 cm^{-1} absorptions, which are the clearest bands of the reaction intermediate, are associated with CH_3 deformation and rocking modes in the $Me_2S : I_2$ van der Waals complex (computed values 1057 and 1363 cm^{-1} respectively).

For the DMS + ICl reaction, again good agreement is obtained between the experimental spectrum and the computed spectrum of the DMS : ICl complex (see Fig. 4). Poor agreement was obtained on comparison of the experimental spectrum with the computed spectra of MClDMS and MIDMS and the product complexes MClDMS : HCl and MIDMS : HCl. Poor agreement was also obtained for the covalent complex Me_2SICl (notably in the 900–1500 cm^{-1} region see Fig. 4 and Table 2). As was the case for the DMS : I_2 complex, the most obvious bands associated with the reaction intermediate at 1040 and 1333 cm^{-1} could be assigned to CH_3 deformation and rocking modes in the Me_2S : ICl van der Waals complex (computed values 1058 and 1365 cm^{-1} respectively). The region 2750–3250 cm^{-1} in Fig. 3 and 4 (the C–H stretching region) is not very helpful in deciding if the experimental spectra are more

Table 4 TDFFT computed vertical singlet-singlet transition energies for the van der Waals complexes DMS : I_2, DMS : ICl and DMS : Br_2 obtained with the CAM-B3LYP functional

(a) DMS : I_2 gas-phase experimental values are given in brackets;[42–44] the weak broad band observed at 457 nm probably has contributions from the first three transitions in this complex.

Transition	Main Excitation HOMO = 42, LUMO = 43	Vertical transition energy/eV	Wavelength/ nm	Oscillator Strength, f
1	42 → 43	2.55 (2.71)	486.6 (457)	0.0014
2	41 → 43	2.56	484.9	0.0009
3	39 → 43	4.04	306.8	0.0023
4	38 → 43	4.05	306.0	0.0001
5	40 → 43	4.63 (4.35)	267.9 (285)	1.0000
6	40 → 44	6.12	202.6	0.0008

(b) DMS : ICl

Transition	Main Excitation HOMO = 38, LUMO = 39	Vertical transition energy/eV	Wavelength/ nm	Oscillator Strength, f
1	38 → 39	3.25	381.3	0.0006
2	37 → 39	3.27	379.0	0.0001
3	35 → 39	5.15	240.4	0.0089
4	34 → 39	5.17	239.9	0.0017
5	36 → 39	5.42	228.9	0.7723
6	36 → 40	6.30	196.9	0.0017

(c) DMS : Br_2

Transition	Main Excitation HOMO = 52, LUMO = 53	Vertical transition energy/eV	Wavelength/ nm	Oscillator Strength, f
1	50 → 53	3.01	412.4	0.0010
2	51 → 53	3.02	410.8	0.0005
3	49 → 53	4.77	259.9	0.1048
4	48 → 53	4.80	258.3	0.0001
5	52 → 53	4.89	253.3	0.9173
6	52 → 54	6.20	200.0	0.0007

appropriately assigned as the van der Waals complex or the covalent complex.

Fig. 1–4 and Tables 1 and 2 show that the infrared spectra of Me_2S : I_2 and Me_2S : ICl are very similar in the 500–3500 cm^{-1} region. They are, however, distinguishable in this region as the bands in the 900–1500 cm^{-1} range are in slightly different positions and they have different relative intensities. For example, in a nitrogen matrix Me_2S : I_2 has three bands at 1331, 1431, and 1441 cm^{-1} which for Me_2S : ICl in the same matrix are observed at 1333, 1432 and 1449 cm^{-1} with different relative intensities.

Discussion

The results of this work show that when DMS and I_2, and DMS and ICl interact and are stabilised by a third body, such as the molecules of an inert gas matrix or the walls of a reaction vessel, van der Waals complexes are formed which have C_1 structures (see Fig. 5). As shown in Table 3, the computed structure of the DMS : I_2 van der Waals complex is very similar to that of the DMS : Br_2 van der Waals complex investigated earlier by infrared matrix isolation and electronic structure calculations.[24] In the DMS + Br_2 study, the three most prominent infrared absorptions that were used to identify the van der Waals complex in matrix isolation experiments were observed in a nitrogen matrix at 204, 1040 and 1332 cm^{-1}.[24] The electronic structure calculations showed that these are associated with a Br–Br···S stretching mode, and CH_3 rocking and deformation modes of the DMS : Br_2 complex. In the case of the DMS : I_2 and DMS : ICl complexes, absorptions were observed corresponding to the CH_3 rocking and deformation modes, but the I–I···S and Cl–I···S stretching modes (expected from *ab initio* calculations at 202 and 176 cm^{-1} respectively) were not observed because of poor signal-to-noise ratios below 250 cm^{-1} in the experimental spectra. It is noted, however, that an I–I···S absorption has been observed for Me_2S : I_2 in a polyethylene matrix at 160 cm^{-1}.[41]

As was found for DMS + Br_2, in the PE experiments that were carried out, no evidence was obtained for complex formation or further reaction. When samples of DMS and I_2 (or ICl) were mixed in the gas-phase at low pressure in an inlet system just above the photoionisation region of the PE spectrometer, no reaction was observed and only DMS and I_2 (or ICl) bands were seen in the spectra. This was because these experiments were carried out at low pressure ($< 10^{-5}$ mbar; time between collisions at 10^{-5} mbar is $\approx 10^{-2}$ s), and at these pressures, the reagents approach, collide and move apart. Stabilisation of the complex by a third body does not occur significantly under these conditions. When pumping on the dark red liquid containing DMS : I_2, only bands of DMS and I_2 were observed in the PE spectra. However in the matrix infrared spectra, bands of DMS and the complex DMS : I_2 were observed, by sampling the vapour above the liquid in the same way. Similar results were obtained on pumping on the brown-orange solid containing DMS : ICl. This must mean that on pumping on these samples, the vapour consists mainly of DMS and I_2 (or ICl) with little complex present. However, when trapped in a matrix, the matrix acts as a third body and the complex (DMS : I_2 or DMS : ICl) is stabilised and hence is observed in the matrix infrared spectra. To study these complexes in the gas-phase by a spectroscopic method such as photoelectron spectroscopy, it is clearly necessary to cool and collisionally stabilise these complexes, for example in a supersonic expansion of the reagents.

Comparison of the minima and transition states computed at the MP2 level for the DMS + I_2 reaction with those computed at the same level for the DMS + Br_2 and DMS + Cl_2 reactions showed that the DMS + I_2 reaction to give MIDMS + HI is endothermic (energy relative to the reagents + 6.0 kcal mol^{-1}) whereas the corresponding DMS + Br_2 and DMS + Cl_2 reactions are exothermic (relative energies (−15.9 and −35.0 kcal mol^{-1} relative to the reagents respectively). On the DMS + I_2 surface, the van der Waals minimum is lower than the covalent minimum (relative energies −11.8 and + 0.5 kcal mol^{-1}) and the barrier to interconvert the van der Waals structure to the covalent structure is very high (+ 28.3 kcal mol^{-1}). In the DMS + Br_2 case, the van der Waals and covalent structures are closer in energy (−11.8 and −12.4 kcal mol^{-1}) and the barrier to conversion from the van der Waals structure to the covalent structure is lower than the DMS + I_2 case but still significant (+ 18.7 kcal mol^{-1}). In the DMS + Cl_2 case, the van der Waals structure is higher in energy than the covalent structure (−9.4 kcal mol^{-1} compared to −24.6 kcal mol^{-1} relative energy) and the barrier for

conversion from the van der Waals form to the covalent form is a lot lower (+ 6.0 kcal mol^{-1}). In the case of DMS + ICl, the overall reaction to give MIDMS + HCl, the lowest energy channel, is exothermic (relative energy −14.6 kcal mol^{-1}). The van der Waals complex is lower in energy than the covalent structure (relative energies −14.5 and −3.3 kcal mol^{-1}) and the barrier to interconversion of the van der Waals structure to the covalent form is high (at +27.4 kcal mol^{-1}). This evidence is consistent with the fact that the DMS : I_2, DMS : ICl and DMS : Br_2 van der Waals complexes could be observed in inert gas matrices by infrared spectroscopy and prepared as stable complexes by mixing the two reagents on a vacuum line. In the DMS + Cl_2 case, the 1 : 1 adduct could not be prepared using standard synthetic methods as mixing the two reagents produced MClDMS + HCl. However, the 1 : 1 adduct was observed in infrared matrix isolation experiments, and the covalent complex was observed in PES experiments performed when sampling the reaction mixture from a flow-tube interfaced to a PE spectrometer.

The computed TDDFT vertical singlet-singlet transition energies from the ground state DMS : XY complexes, with XY = I_2, ICl and Br_2 are shown in Table 4.

In each case, as can be seen from the computed oscillator strengths in Table 4, the first transition is quite weak and the fifth transition is the most intense. The only DMS : XY complex to have been investigated in the gas-phase by electronic absorption spectroscopy is DMS : I_2. This shows a weak broad band centred at 2.712 eV (457 nm) and a more intense broad band at 4.35 eV (285 nm).[42–44] At the time that this work[42–44] was carried out, the first band was thought to be due to a valence transition and the stronger band was thought to be a DMS to XY electron transfer transition. Inspection of the main excitations associated with each transition in the TDDFT calculations shows that the most intense singlet-singlet transition (the fifth transition in each case) does indeed consist of a DMS to XY transition from a delocalised molecular orbital, which is mainly on the DMS moiety and is S–X bonding and X–Y antibonding, to an orbital which is mainly localised on the X–Y moiety and is X–Y and S–X antibonding. This transition is therefore expected to weaken the X–Y bond as well as the S–X bond. In contrast, the lowest energy singlet-singlet transition consists of an XY to DMS transition from an antibonding orbital on the XY unit to a delocalised orbital over the S, X and Y centres which is X–Y and S–X antibonding. This is expected to weaken the DMS–XY bond but not the X–Y bond in DMS : XY.

As can be seen from Table 4, the general trend observed on going from ICl to Br_2 to I_2 is that the transitions move to lower energy. In particular, the most intense transition, the DMS to XY charge transfer transition, moves from 5.42 eV (229 nm) to 4.89 eV (253 nm) to 4.63 eV (285 nm).

The atmospheric relevance of this work is that the DMS : halogen complexes studied could well be a reservoir of halogen molecules in the atmosphere which will contribute to ozone depletion.[45] For example, the DMS : I_2 and DMS : ICl complexes will be stabilised on cold surfaces such as on ice surfaces or aerosols. On warming, DMS and I_2 (or ICl) will be released. These complexes could therefore act as reservoirs for diatomic halogens in the atmosphere which on photodissociation by radiation from the sun will give halogen atoms which lead to ozone depletion. Also, exposure of DMS : I_2 and DMS : ICl trapped on cold surfaces to sunlight at wavelengths less than 300 nm, could result in photodissociation of the halogen moiety, which will lead to enhancement of ozone depletion. This is very reasonable as in the polar tropospheric boundary layer, it has been established that reactive halogen species are responsible for ozone destruction as well as oxidation of DMS. After polar sunrise, air masses enriched in reactive halogen species are known to cover large areas. However, the source and release mechanisms of these reactive halogen species have not been established.[46–48]

Conclusions

The reactions of I_2 and ICl with DMS have been studied using infrared matrix isolation spectroscopy and electronic structure calculations. These studies show that these reactions do not proceed further than the van der Waals complexes, DMS : I_2 and DMS : ICl, which were observed in the matrix isolation experiments. This result is consistent with that observed earlier for the DMS + Br_2 reaction, but different from the DMS + Cl_2 case which proceeds further to a covalent complex and then on to the final products, MClDMS + HCl. These observations are supported by the results of the MP2 calculations. The importance of the results obtained to atmospheric chemistry has also been considered, notably their possible relevance to halogen atom catalysed ozone depletion.

This study is currently being extended by considering the reactions of DMS with halogens in the presence of a water molecule, and the reactions of DMSe with halogens.

Acknowledgements

SB and NA thank the EU Early Stage Research Training Network (SEACHERS) for financial support. JMD thanks the Leverhulme Trust for an Emeritus Fellowship. The authors also acknowledge support from the UK National Service in Computational Chemistry Software (NSCCS). This paper is dedicated to Steve Ogden, our friend, colleague and co-author who sadly passed away during the preparation of this paper.

References

1 R. J. Charlson, J. E. Lovelock, M. O. Andreae and S. G. Warren, *Nature*, 1987, **326**, 655.
2 S. F. Watts, *Atmos. Environ.*, 2000, **34**, 761.
3 T. S. Bates, B. K. Lamb, A. Guenther, J. Dignon and R. E. Stoiber, *J. Atmos. Chem.*, 1992, **14**, 315.
4 H. Berresheim, P. H. Wine and D. D. Davis, in *"Composition, Chemistry and Climate of the Atmosphere"*, van Nostrand Reinhold, New York, 1995, p. 251.
5 S. E. Schwarz, *Nature*, 1988, **336**, 441.
6 C. F. Cullis and M. M. Hirschler, *Atmos. Environ.*, 1980, **14**, 1263.
7 T. S. Bates, J. D. Cline, R. H. Gammon and S. R. Kelly-Hansen, *J. Geophys. Res.*, 1987, **92**, 2930.
8 A. R. Ravishankara, Y. Rudich, R. Talukdar and S. B. Barone, *Philos. Trans. R. Soc. London, Ser. B*, 1997, **352**, 171.
9 J. B. Novak, D. D. Davis, G. Chen, F. L. Eisele, R. L. Mauldin, D. J. Tanner, C. Cantrall, E. Koscuich, A. Bandy, D. Thornton and A. Clarke, *Geophys. Res. Lett.*, 2001, **28**, 2201.
10 M. O. Andreae and P. J. Crutzen, *Science*, 1997, **276**, 1052.
11 R. Vogt, P. J. Crutzen and R. Sander, *Nature*, 1996, **383**, 327.

12 A. Saiz-Lopez and J. M. C. Plane, *Geophys. Res. Lett.*, 2004, **31**, L04112.
13 A. Saiz-Lopez, A. S. Mahajan, R. A. Salmon, S. J. B. Baugitte, A. E. Jones, H. K. Roscoe and J. M. C. Plane, *Science*, 2007, **317**, 348.
14 Y. Sakamoto, A. Yabushita, M. Kawasaki and S. Enami, *J. Phys. Chem. A*, 2009, **113**, 7707.
15 J. A. Garland and H. Curtis, *J. Geophys. Res.*, 1981, **86**, 3183.
16 D. O'Sullivan and J. R. Sodeau, *J. Phys. Chem. A*, 2010, **114**, 12208.
17 P. O'Driscoll, K. Lang, N. Minoque and J. Sodeau, *J. Phys. Chem. A*, 2006, **110**, 4615.
18 J. Abbatt, N. Oldridge, A. Symington, V. Chukalovsky, R. D. McWhinney, S. Sjostedt and R. A. Cox, *J. Phys. Chem. A*, 2010, **114**, 6527.
19 S. Hayase, A. Yabushita and M. Kawasaki, *J. Phys. Chem. A*, 2011, **115**, 4935.
20 R. B. Chatfield and P. J. Crutzen, *J. Geophys. Res.*, 1990, **95**, 22319.
21 L. J. Carpenter, *Chem. Rev.*, 2003, **103**, 4953.
22 J. M. Dyke, M. V. Ghosh, D. J. Kinnison, G. Levita, A. Morris and D. E. Shallcross, *Phys. Chem. Chem. Phys.*, 2005, **7**, 866.
23 J. M. Dyke, M. V. Ghosh, M. Goubet, E. P. F. Lee, G. Levita, K. Miqueu and D. E. Shallcross, *Chem. Phys.*, 2006, **324**, 85.
24 S. Beccaceci, J. S. Ogden and J. M. Dyke, *Phys. Chem. Chem. Phys.*, 2010, **12**, 2075.
25 J. S. Ogden and R. Wyatt, *J. Chem. Soc., Dalton Trans.*, 1987, 859.
26 J. M. Dyke, N. Jonathan and A. Morris, *Electron Spectroscopy*, Academic Press, London 1979, vol. 3, p. 189.
27 J. M. Dyke, A. Morris and N. Jonathan, *Int. Rev. Phys. Chem.*, 1982, **2**, 3.
28 K. Kimura, S. Katsumata, Y. Achiba, T. Yamazaki and S. Iwata, *Handbook of HeI Photoelectron Spectra, Japan*, Scientific Societies Press, Halstead Press, Tokyo, 1981.
29 A. B. Cornford, D. C. Frost, C. A. MacDowell, J. L. Ragle and I. A. Stenhouse, *J. Chem. Phys.*, 1971, **54**, 2651.
30 A. W. Potts and W. C. Price, *Trans. Faraday Soc.*, 1971, **67**, 1242.
31 S. Evans and A. F. Orchard, *Inorg. Chim. Acta*, 1971, **5**, 81.
32 M. J. Frisch, G. W. Trucks, H. B. Schlegel, G. E. Scuseria, M. A. Robb, J. R. Cheeseman, J. A. Montgomery, Jr., T. Vreven, K. N. Kudin, J. C. Burant, J. M. Millam, S. S. Iyengar, J. Tomasi, V. Barone, B. Mennucci, M. Cossi, G. Scalmani, N. Rega, G. A. Petersson, H. Nakatsuji, M. Hada, M. Ehara, K. Toyota, R. Fukuda, J. Hasegawa, M. Ishida, T. Nakajima, Y. Honda, O. Kitao, H. Nakai, M. Klene, X. Li, J. E. Knox, H. P. Hratchian, J. B. Cross, V. Bakken, C. Adamo, J. Jaramillo, R. Gomperts, R. E. Stratmann, O. Yazyev, A. J. Austin, R. Cammi, C. Pomelli, J. W. Ochterski, P. Y. Ayala, K. Morokuma, G. A. Voth, P. Salvador, J. J. Dannenberg, V. G. Zakrzewski, S. Dapprich, A. D. Daniels, M. C. Strain, O. Farkas, D. K. Malick, A. D. Rabuck, K. Raghavachari, J. B. Foresman, J. V. Ortiz, Q. Cui, A. G. Baboul, S. Clifford, J. Cioslowski, B. B. Stefanov, G. Liu, A. Liashenko, P. Piskorz, I. Komaromi, R. L. Martin, D. J. Fox, T. Keith, M. A. Al-Laham, C. Y. Peng, A. Nanayakkara, M. Challacombe, P. M. W. Gill, B. Johnson, W. Chen, M. W. Wong, C. Gonzalez and J. A. Pople, *GAUSSIAN 03 (Revision C.02)*, Gaussian, Inc., Wallingford, CT, 2004.
33 C. Moller and M. Plesset, *Phys. Rev.*, 1934, **46**, 618.
34 D. E. Woon and T. H. Dunning, *J. Chem. Phys.*, 1993, **98**(2), 1358.
35 (*a*) http://www.emslpnl.gov/forms/basisform.html; (*b*) K. A. Peterson, D. Figgen, E. Goll, H. Stoll and M. Dolg, *J. Chem. Phys.*, 2003, **119**, 11113.
36 T. Yanai, D. P. Tew and N. C. Handy, *Chem. Phys. Lett.*, 2004, **393**, 51–57.
37 M. J. G. Peach, P. Benfield, T. Helgaker and D. J. Tozer, *J. Chem. Phys.*, 2008, **128**, 044118.
38 M. J. Peach, T. Helgaker, P. Salek, T. W. Keal, O. B. Lutnaes, D. J. Tozer and N. C. Handy, *Phys. Chem. Chem. Phys.*, 2006, **8**, 558.
39 D. Jacquemin, E. A. Perpete, G. E. Scuseria, I. Ciofini and C. Adamo, *J. Chem. Theory Comput.*, 2008, **4**, 123.
40 M. Ghosh, J. S. Ogden and J. M. Dyke, unpublished work.
41 M. Yamada, H. Saruyama and K. Aida, *Spectrochim. Acta*, 1972, **28A**, 439.
42 M. Tamres and S. N. Bhat, *J. Am. Chem. Soc.*, 1972, **94**, 2577.
43 M. Tamres and S. N. Bhat, *J. Phys. Chem.*, 1971, **75**, 1057.
44 M. Kroll, *J. Am. Chem. Soc.*, 1968, **90**, 1097.
45 D. J. Lary, *J. Geophys. Res.*, 1996, **101**, 1505.
46 D. Poehler, L. Vogel, U. Friess and U. Platt, *Proc. Natl. Acad. Sci. U. S. A.*, 2010, **107**(15), 6582–6587.
47 D. Helmig, E. Apel, D. Blake, L. Ganzeveld, B. L. Lefer, S. Meinardi and A. L. Swanson, *Biogeochemistry*, 2009, **95**, 167.
48 K. A. Read, A. S. Mahajan, L. J. Carpenter, M. J. Evans, B. V. E. Faria, D. E. Heard, J. R. Hopkins, J. D. Lee, S. J. Moller, A. C. Lewis, L. Mendes, J. B. McQuaid, H. Oetjen, A. Saiz-Lopez, M. J. Pilling and J. M. C. Plane, *Nature*, 2008, **453**, 1232.